For submission to Water Science and Technology as a Research Paper

High spatial resolution analysis of the distribution of sulfate reduction and sulfide oxidation in hypoxic sediment in a eutrophic estuary

Short title

High spatial resolution analysis of H_2S in sediment

Rathnayake M.L.D. Rathnayake[a], Shogo Sugahara[b], Hideaki Maki[c], Gen Kanaya[c], Yasushi Seike[b], and Hisashi Satoh[d,*]

[a] Department of Civil Engineering, Faculty of Engineering, University of Peradeniya, 20400, Sri Lanka

[b] Interdisciplinary Faculty of Science and Engineering, Shimane University, Matsue, Shimane 690–8504, Japan

[c] National Institute for Environmental Studies (NIES), 16-2, Onogawa, Tsukuba, Ibaraki 305–8506, Japan

[d] Division of Environmental Engineering, Faculty of Engineering, Hokkaido University, North-13, West-8, Sapporo 060–8628, Japan

*Corresponding author

Hisashi Satoh

Division of Environmental Engineering, Faculty of Engineering, Hokkaido University, North-13, West-8, Sapporo 060-8628, Japan

Tel: +81-(0)11-706-6277, Fax: +81-(0)11-706-6277, E-mail: qsatoh@eng.hokudai.ac.jp

ABSTRACT

Bottom hypoxia and consequential hydrogen sulfide (H_2S) release from sediment in eutrophic estuaries is a major global environmental issue. We investigated dissolved oxygen, pH and H_2S concentration profiles with microsensors and by sectioning sediment

cores followed by colorimetric analysis. The results of these analyses were then compared with the physicochemical properties of the bottom water and sediment samples to determine their relationships with H_2S production in sediment. High organic matter and fine particle composition of the sediment reduced the oxidation-reduction potential, stimulating H_2S production. Use of a microsensor enabled measurement of H_2S concentration profiles with submillimeter resolution, whereas the conventional sediment-sectioning method gave H_2S measurements with a spatial resolution of 10 mm. Furthermore, microsensor measurements revealed H_2S consumption occurring at the sediment surface in both the microbial mat and the sediment anoxic layer that were not observed with sectioning. This H_2S consumption prevented H_2S release into the overlying water. However, the microsensor measurements had the potential to underestimate H_2S concentrations. We propose that a combination of several techniques to measure microbial activity and determine its relationships with physicochemical properties of the sediment is essential to understanding the sulfur cycle under hypoxic conditions in eutrophic sediments.

Keywords: Concentration profiles; Microsensors; Particle composition; Physicochemical properties; Sediment core sectioning; White filamentous bacteria

Introduction

Eutrophication caused by anthropogenic activity is a major environmental problem in estuaries. In particular, urbanized and industrialized watersheds can result in large inputs of organic matter and nutrients into estuaries. Degradation of organic matter in an estuary results in reduction or complete depletion of dissolved oxygen (DO) in the bottom water, which are termed hypoxia and anoxia, respectively (Kodama et al. 2010; Sato et al. 2012). Low DO can lead to increased mortality of macrobenthic fauna and fish, as well as to accelerated production of hydrogen sulfide (H_2S) in hypoxic bottom sediments (Valdemarsen et al. 2009). Because H_2S is both toxic to benthic biota and consumes DO, H_2S production is harmful to estuarine ecosystems and should be prevented (Kodama et al. 2010). However, the mechanism of H_2S production is complicated and depends on sediment physicochemical properties including DO, oxidation-reduction potential (ORP),

pH, nitrate, sulfate and organic matter concentrations, as well as sediment grain size and porosity (Valdemarsen et al. 2009); therefore, it is difficult to control.

To understand the mechanism of H_2S production, H_2S concentration profiles in the sediment have been examined using several different techniques. Traditionally, H_2S profiles have been determined by sectioning sediment cores and performing colorimetric H_2S determination of interstitial water samples obtained by squeezing or *in situ* equilibration of dialysis cells (Koretsky et al. 2007). However, the difficulties associated with fine scale sediment sectioning result in a spatial resolution of only a few centimeters. At the sediment-water interface, steep concentration gradients can exist at a submillimeter scale, making the sectioning technique inadequate (Nakamura et al. 2004). Therefore, other analytical methods with higher spatial resolution (e.g., diffusive equilibration [DET] and diffusive gradients in thin-films [DGT], planar optodes and microsensors) have been developed and used for the measurement of H_2S concentration profiles. DET and DGT techniques are used to investigate the two-dimensional distribution of H_2S in the sediment. In these methods, H_2S diffusing into thin hydrogel is trapped by an immobilized binding agent, then subjected to colorimetric determination (Pages et al. 2014). These techniques typically have a spatial resolution in the millimeter scale (Gregusova & Docekal 2013); however, they require labor-intensive and time-consuming steps such as gel preparation and several days of gel deployment for equilibration and H_2S determination. Planar optodes allow two-dimensional measurements of dissolved matter at higher spatial (micrometer) and temporal (minutes) resolution than either the DET or DGT technique. Planar optodes have been used to determine the two-dimensional distribution and dynamics of DO and pH (Larsen et al. 2011) and CO_2 (Zhu & Aller, 2010) in both sediment and soil. However, the types of fluorescent indicators available for planar optodes are limited; therefore, they can only be used for a few analytes (Glud 2008).

Microsensors, which have been developed for a variety of analytes in the last three decades, may provide a solution to the shortfalls of the previous methods. Microsensors are biochemical sensors with a tip having a diameter at the micrometer scale. Because of their small size, microsensors have been used to determine the concentration profiles of dissolved matter with minimal disturbance of the sediment sample. Revsbech et al. (1980),

who was the first to use an oxygen (O_2) microsensor for sediment analysis, revealed the steep concentration gradients of DO and heterogeneity of its distribution. Since then, various types of microelectrodes have been developed and introduced to determine concentration profiles of H_2S (Kühl et al. 1998), N_2O (Binnerup et al. 1992) and metals (Luther et al. 1998) in lake, estuary and continental shelf sediments. However, no studies have investigated the relationship between the measured H_2S concentration profile and the physicochemical properties of hypoxic and/or anoxic sediment in eutrophic estuaries. An understanding of the relationship between H_2S production and consumption with the physicochemical properties of the water-sediment interface is essential for the prevention of H_2S release and subsequent hypoxia in the sediment. In this study, DO, pH and H_2S concentration profiles at the water-sediment interface of hypoxic sediment were monitored by microsensors. H_2S concentration profiles in the sediment samples were determined using the H_2S microsensor and by sectioning sediment cores and then subjecting the sections to colorimetric analysis. The sediment samples were obtained from Tokyo Bay because previous studies have demonstrated that eutrophication causes hypoxia from spring to autumn in this system (Sato et al. 2012). H_2S profiles were compared with physicochemical properties of the sediment samples to better understand the role of sediment physicochemistry in the sulfur cycle.

Materials and methods

Samples

Samples of overlying water and sediments were collected from three sites in Tokyo Bay between May 2010 and August 2011: the Chiba Light Beacon vicinity (34°34′05″N, 140°2′45″E, 12–13 m water depth), Sanmaizu (35°36′53″N, 139°51′34″E, 6–7 m water depth) and the Tokyo Light Beacon (35°34′9″N, 139°50′51″E, 15–16 m water depth), hereafter referred to as Sites 1, 2 and 3, respectively (Figure 1). Vertical profiles of the physicochemical parameters (DO, temperature and salinity) in the bottom water were obtained *in situ* using a sounder (Hydrolab DataSonde 4a; Hach Environmental, Loveland, CO, USA). Oxidation-reduction potential (ORP) was measured with a glass electrode (9300-10D, Horiba, Kyoto, Japan).

Sediment cores were sampled *in situ* using acrylic tubes (4 cm inner diameter, 40 cm in length) inserted directly into the sediment by divers. After plugging both ends of the acrylic tubes with rubber lids, the tubes were transported onto boats and stored in cooling boxes until laboratory analysis. Sediment grain size and composition were determined using the sieving and precipitation method following the test method for particle size distribution of soil (Japanese Industrial Standards [JIS] A 1204:2009 and Japanese Geotechnical Society [JGS] 0131-2009) described in the Laboratory Testing Standards of Geomaterials published by the JGS. Sediments were dried to constant weight at 105°C (approximately 2 h) to determine water content (%). Subsamples (approximately 1 g) were burned for 2 h at 650°C to determine loss on ignition (LOI). Acid volatile sulfide (AVS) content in the sediment samples was assayed using HYDROTEC-S (GASTEC, Japan). Briefly, approximately 1 g wet sediment was transferred into a glass vessel, which acted as a H_2S gas generation tube, to which 2 mL of 18 N sulfuric acid was added. The H_2S gas generated was then drawn into a H_2S detecting tube by suction via a sealed glass cap and a gas sampling pump. The ORP and temperature were measured directly by inserting a glass electrode into the sediment samples.

Colorimetric determination of H_2S in interstitial water of the sediment samples

Colorimetric determination of dissolved sulfide, which was defined as the sum of H_2S, HS^- and S^{2-}, was accomplished according to the modified methods of Cline 1969 (Sugahara et al. 2010). The sulfide concentration measured using this method was referred to as $\Sigma(H_2S)$. Each sediment core was horizontally sliced 1, 2 and 3 cm from the top of the core by stepwise extrusion from the corer using a plunger. Each sediment slice was then placed in a plastic cup, and a sample was immediately taken using a 30 mL glass syringe. The samples were volumetrically adjusted to 2.5 mL, after which 20 mL of N_2 gas-purged, DO-free deionized water was added directly to each syringe via a three-way stopcock. The sediment samples were suspended in the deionized water by manual shaking after ejecting the air from the syringes. Each suspended sediment sample was then filtered with a cellulose acetate membrane filter cartridge (25 mm diameter, 0.45 μm pore size, DISMIC-25CS, Advantec, Japan), and 10 mL filtrate was introduced into a new syringe via

a three-way stopcock. One milliliter of 0.23 M zinc acetate solution was then added directly to the filtrate in each syringe to form zinc sulfide, after which 2 mL of 6 N hydrochloric acid solution was added to the zinc sulfide, and the $\Sigma(H_2S)$ concentration was determined using methylene blue. This process involves the addition of 0.5 mL coloring reagent (a mixture of N,N-dimethyl p-phenylene diamine sulfate [DMPDS] and ferric chloride [$FeCl_3$]) to the acidified samples, which are then rested for 15 minutes to allow the formation of methylene blue as a chromophore. The methylene blue concentration was then determined by spectrophotometry at a wavelength of 667 nm 2 hours after the addition of DMPDS solution. Two types of coloring reagent solutions were used according to the $\Sigma(H_2S)$ concentration: (1) 0.4 g of DMPDS and 0.6 g of $FeCl_3 \cdot 6H_2O$ containing 100 mL of 6 N HCl for low $\Sigma(H_2S)$ concentration samples (<2 mg $\Sigma(H_2S)$ L^{-1}) and (2) 4.0 g of DMPDS and 6.0 g of $FeCl_3 \cdot 6H_2O$ containing 100 mL of 6 N HCl for high $\Sigma(H_2S)$ concentration samples (<30 mg $\Sigma(H_2S)$ L^{-1}). Determination of high $\Sigma(H_2S)$ concentration samples required dilution of the methylene blue solution with deionized water to adjust the concentration to within the quantitative range of absorbance values measureable by the spectrophotometer.

Microsensor measurements

Steady-state concentration profiles of DO, T-H_2S ($\Sigma(H_2S)$ measured with a H_2S microsensor) and pH were measured according to the method described by Okabe et al. (1999). Clark-type O_2 and H_2S microsensors and a pH microsensor were purchased from Unisense (Arhus, Denmark) and calibrated according to the manufacturer instructions. DO, T-H_2S and pH concentration profiles in the sediment samples were obtained using a micromanipulator at intervals of 200 to 500 μm. The microsensor tip was positioned with a dissecting microscope (model Stemi 2000; Carl Zeiss). Three concentration profiles for each species were measured at different points in each sediment sample.

The net volumetric T-H_2S production rate (R(T-H_2S)) in each sediment sample was calculated from the mean steady-state concentration profiles of T-H_2S using Fick's second law of diffusion as described by Okabe et al. (1999):

$$\frac{dC(x,t)}{dt} = D_s \frac{d^2C(x,t)}{dx^2} + R(x)$$

where, C is the concentration of the chemical species at depth x and time t, Ds is the sediment diffusion coefficient of the chemical species, and R is the production rate of the chemical species at depth x. Positive and negative values of R(T-H_2S) indicate T-H_2S production (i.e., sulfate reduction) and consumption, respectively. We used the Ds values previously determined in sediments: $Ds(O_2) = 1.31\times10^{-5}$ cm^{-2} s^{-1} (Nakamura et al. 2004) and $Ds(H_2S) = 1.39\times10^{-5}$ cm^{-2} s^{-1} (Okabe et al. 1999). The rates were calculated as described previously by Okabe et al. (1999). The local diffusive fluxes of T-H_2S (J(T-H_2S)) and DO ($J(O_2)$) were calculated using Fick's first law of diffusion (Okabe et al. 1999):

$$J(x) = -\Phi D_s \frac{dC(x)}{dx}$$

where, Φ is the sediment porosity measured in this study.

To examine the effectiveness of each method of sulfide measurement, the ratio of sulfide determined by the microsensor (quantity of T-H_2S) to that determined by colorimetric determination (quantity of $\Sigma(H_2S)$) was calculated. The quantity of T-H_2S was estimated by integrating the T-H_2S concentration profile over a depth of 10 mm, while that of $\Sigma(H_2S)$ was estimated as $\Sigma(H_2S)$ multiplied by 10 mm of depth.

Results

Physicochemical properties of the sediment and bottom water

The average percentage of sand, silt and clay in the sediment samples taken from three sites in the inner Tokyo Bay between May 2010 and August 2011 (n = 9) are shown in Table 1. The samples were taken at a sediment depth of 0.1 m. In Sites 1 and 3, the sediment was mainly composed of silt and clay, whereas sand comprised 52% of the sediment in Site 2.

The physicochemical properties of the bottom water and of the sediment samples at a sediment depth of 3 cm for each of the three study sites are shown in Table 2. Sediment AVS concentrations were higher and ORP values were lower at Site 3 than at Sites 1 or 2. Loss on ignition, which is an indicator of organic matter content, was higher at Site 3 than at the other sites. Sediment water content was high at Sites 1 and 3, but low at Site 2, indicating more extensive dewatering and compaction of the sediment at Site 2. DO in the bottom water was below 15 μM (0.5 mg L^{-1}) at all sites on all three sampling dates, except for Site 2 on July 2010 (37 μM), when ORP in the bottom water was also much higher (+165 mV) than at other sites or other times. Overall, sediment AVS concentrations were relatively high at Site 3, which was characterized by fine sediments, lower ORP and higher LOI.

Vertical distribution of H_2S concentrations and rates of sulfate reduction and sulfide oxidation at the sediment surface

The vertical distribution of bulk $\Sigma(H_2S)$ at the sediment surface of each site was determined by the colorimetric method (Figure 2). Bulk $\Sigma(H_2S)$ concentrations increased with depth in all samples. Bulk Σ (H_2S) concentrations in the deepest layer (i.e., 20–30 mm depth) of the sediment were highest at Site 3 (2,000–12,000 μM) and lowest at Site 2 (<250 μM). AVS concentrations followed a similar trend among sites (Table 2).

The steady-state concentration profiles of DO, T-H_2S and pH measured with microsensors are depicted in Figure 2. DO was depleted at the sediment surface in most samples; thus, DO profiles are only shown for Sites 1 and 2 on July 2010 (Figure 2A and B). DO penetrated only 0.4 mm into the sediment at Site 2 on July 2010 (Figure 2A), even when the DO of the bottom water was 100 μM. DO depletion was likely caused by a combination of high microbial respiration during oxidation of organic matter, low DO in the bottom water, low liquid flow rate at the sediment surface during measurement, and/or fine silt or clay particles inhibiting DO diffusion into the sediment. $J(O_2)$ fluxes, which were calculated from the linear DO concentration profiles at the sediment surface, were 0.049 and 0.045 μmol cm^{-2} h^{-1} at Sites 1 and 2, respectively, on July 2010. Because the

samples were incubated in the dark, DO showed no net increase, indicating insignificant photosynthesis in all samples. These reducing conditions resulted in sulfate reduction in the sediment. The T-H_2S concentrations increased with depth at all three sites, although they were higher at Sites 1 and 3 (~2,700 μM) than at Site 2 (<600 μM) on each sampling date. The T-H_2S concentrations were highest on August 2010 for all samples.

The standard deviation of the T-H_2S concentration at each sediment depth was lower than 5%, except for Site 2 on August 2010 (<20%) and August 2011 (<60%). These findings indicate that the vertical distribution of sulfate reduction and sulfide oxidation was relatively homogenous. Therefore, the net volumetric T-H_2S production rates (R(T-H_2S)) were calculated from the average steady-state concentration profiles of T-H_2S by diffusion reaction modeling (Figure 3). In addition, the local diffusive fluxes of T-H_2S (J(T-H_2S)) were calculated from the linear T-H_2S concentration profiles of the measured sediment depth range (Table 3). R(T-H_2S) in Sites 1 and 3 on August 2010 were relatively high (<0.26 μmol cm^{-3} h^{-1}), resulting in high J(T-H_2S) in these samples (Table 3). Thus, significant concentrations of H_2S were detected in the bottom waters at Site 1 (0.02 mg S L^{-1}) and Site 3 (0.74 mg S L^{-1}). In some sediment samples, rates of T-H_2S oxidation were so low that T-H_2S reached the sediment surface (Table 3) and diffused into the overlying water (Figure 2). In contrast, at Sites 1 and 3 on July 2010 and Site 2 on August 2010, T-H_2S was completely oxidized at the surface sediment (Table 3). H_2S oxidation at the surface sediment is vital for preventing toxic H_2S release from the sediment into the overlying water.

Discussion

Among the study sites in Tokyo Bay, sulfate reduction, which was represented by AVS, bulk Σ(H_2S) and T-H_2S accumulation, was highest at Site 3 on each sampling date. Moreover, Site 3 was characterized by higher LOI (organic matter) than Sites 1 or 2 (Table 2). High organic matter in the sediment can stimulate sulfate reduction via consumption of DO followed by a decrease in ORP in sediment or by providing increased quantities of electron donors for sulfate-reducing bacteria (Holmer & Storkholm 2001). Rates of sulfate reduction (R(T-H_2S)) in this study (<0.26 μmol cm^{-3} h^{-1}) were substantially higher than

those of natural sediments in acidic lakes (Kühl et al. 1998) and sandy intertidal sediments (de Beer et al. 2005) (<0.01 μmol cm^{-3} h^{-1}), while they were comparable to those of anaerobic sewer biofilm (Mohanakrishnan et al. 2009) and organic-rich sludge in a marine aquaculture system (Schwermer et al. 2010) (<1.0 μmol cm^{-3} h^{-1}). Thus, these results indicate a massive input of organic matter to Tokyo Bay sediments is occurring. Moreover, the fine particles comprising the sediment at Site 3 may reduce the diffusive transport of oxygenated species (e.g., DO, nitrate and ferric oxide) and eventually stimulate sulfate reduction. Kodama et al. (2010) also reported severe bottom hypoxia (<45 μM of DO) in a northern area of Tokyo Bay, including all sites in this study in August 2005, and found H_2S concentrations were higher in silt and clay sediments than in sand.

Comparison of the T-H_2S concentration profiles measured by a microsensor with the vertical distribution of bulk Σ(H_2S) demonstrated that T-H_2S could be determined at depth intervals of 0.2 mm, whereas bulk Σ(H_2S) concentration intervals were 10 mm. The microsensor measurements showed that T-H_2S concentrations were changing at the submillimeter scale. It should be noted that the T-H_2S was completely oxidized at a depth of 5.5 mm in the Site 3 sediment on July 2010, and that no T-H_2S was detected in the surface layer of the sediment, but a microbial mat of white filamentous bacteria approximately 10 mm thick was found on the sediment surface (Figure 4). This was likely to consist of *Beggiatoa* spp., which can oxidize H_2S with DO and/or nitrate (Kamp et al. 2006). It is well known that mats of *Beggiatoa* at the sediment surface can prevent the diffusion of toxic H_2S into overlying waters because biological H_2S oxidation is much more rapid and efficient than chemical H_2S oxidation (Kamp et al. 2006). DO was depleted at the sediment surface because of low DO in the bottom water layer, and the sum of nitrate and nitrite concentrations in the bottom water was only 6 μM at Site 3 on July 2010. In addition, electric currents may not have directly connected oxygen reduction at the sediment surface to sulfide oxidation at deeper sediment depths in this sample, as pH was observed to increase between the oxygen reduction and sulfide oxidation zones (Pfeffer et al. 2012). Therefore, an electron acceptor for *Beggiatoa*-like bacteria has not been identified. Furthermore, a decrease in T-H_2S concentrations was observed in anoxic sediments deeper than 3 mm at Site 2 on August 2011. Decreased T-H_2S may have been caused by bioturbation providing oxygen and/or nitrate (Rabouille et al. 2009) or by upward diffusion

of dissolved Fe^{2+} reacting with H_2S to form FeS under reducing conditions in the sediment (Dittrich et al. 2009). Without the use of a microsensor, these unusual phenomena would have been overlooked.

T-H_2S and bulk $\Sigma(H_2S)$ concentration profiles showed some similarities; specifically, both increased with sediment depth and were lower in sediments at Site 2 than at Sites 1 or 3. However, the ratio of the quantity of T-H_2S to bulk $\Sigma(H_2S)$ in the top 10 mm of sediment ranged from 0.01 to 10 (Table 3), indicating that microsensor measurements may frequently underestimate H_2S concentrations. Although the exact reason remains unknown, one explanation may be that T-H_2S concentration profiles were measured in the laboratory under different conditions than those *in situ*. Alternatively, the T-H_2S concentration profiles may not necessarily represent an averaged concentration profile because of inadequate replication (only 3 points per sediment sample). Nevertheless, our results indicate that microsensor measurement is necessary to properly analyze the sulfur cycle in sediment at the submillimeter scale.

Conclusions

The H_2S concentration profiles and rates of sulfate reduction and sulfide oxidation in the sediment of Tokyo Bay were determined at a submillimeter scale using a microsensor, whereas the spatial resolution of the sediment core sectioning method was 10 mm. The calculated T-H_2S production rates in some eutrophic sediment samples were much higher than those found in natural sediments in other studies. Among the sediment properties measured, high organic matter content and fine particle composition (i.e., silt and clay) may primarily be responsible for the inhibition of DO diffusion into the sediment, the low ORP and the stimulation of sulfate reduction at the surface sediment in Tokyo Bay. Sulfate reduction and H_2S oxidation in the sediment showed dynamic variation with depth at the submillimeter scale and differed among sites. Without the use of a microsensor, these spatial dynamics with depth would have been overlooked. Overall, microsensor measurements provided critical insight into the sulfur cycle in the hypoxic surface sediment of a eutrophic estuary.

References

de Beer, D., Wenzhöfer, F., Ferdelman, T. G., Boehme, S. E., Huettel, M., van Beusekom, J. E. E., Böttcher, M. E., Musat, N., and Dubilier, N. (2005) Transport and mineralization rates in North Sea sandy intertidal sediments, Sylt-Rømø Basin, Waddensea. Limnology and Oceanography, **50**(1), 113–127.

Binnerup, S. J., Jensen, K., Revsbech, N. P., Jensen, M. H., and Sorensen, J. (1992) Denitrification, dissimilatory reduction of nitrate to ammonium, and nitrification in a bioturbated estuarine sediment as measured with 15N and microsensor techniques. Applied and Environmental Microbiology, **58**(1), 303–313.

Cline, J. D. (1969) Spectrophotometric determination of hydrogen sulfide in natural waters. Limnology and Oceanography, **14**(3), 454–458.

Dittrich, M., Wehrli, B., and Reichert, P. (2009) Lake sediments during the transient eutrophication period: Reactive-transport model and identifiability study. Ecological Modelling, **220**(20), 2751–2769.

Glud, R. N. (2008) Oxygen dynamics of marine sediments. Marine Biology Research, **4**(4), 243–289.

Gregusova, M. and Docekal, B. (2013) High resolution characterization of uranium in sediments by DGT and DET techniques ACA-S-12-2197. Analytica Chimica Acta, **763**, 50–56.

Holmer, M. and Storkholm, P. (2001) Sulphate reduction and sulphur cycling in lake sediments: A review. Freshwater Biology, **46**(4), 431–451.

Kamp, A., Stief, P., and Schulz-Vogt, H. N. (2006) Anaerobic sulfide oxidation with nitrate by a freshwater Beggiatoa enrichment culture. Applied and Environmental Microbiology, **72**(7), 4755–4760.

Kodama, K., Oyama, M., Kume, G., Serizawa, S., Shiraishi, H., Shibata, Y., Shimizu, M., and Horiguchi, T. (2010) Impaired megabenthic community structure caused by summer hypoxia in a eutrophic coastal bay. Ecotoxicology, **19**(3), 479–492.

Koretsky, C. M., Haveman, M., Beuving, L., Cuellar, A., Shattuck, T., and Wagner, M. (2007) Spatial variation of redox and trace metal geochemistry in a minerotrophic fen. Biogeochemistry, **86**(1), 33–62.

Kühl, M., Steuckart, C., Eickert, G., and Jeroschewski, P. (1998) A H2S microsensor for profiling biofilms and sediments: Application in an acidic lake sediment. Aquatic Microbial Ecology, **15**(2), 201–209.

Larsen, M., Borisov, S. M., Grunwald, B., Klimant, I., and Glud, R. N. (2011) A simple and inexpensive high resolution color ratiometric planar optode imaging approach: application to oxygen and pH sensing. Limnology and Oceanography: Methods, **9**, 348–360.

Luther, G. W., Brendel, P. J., Lewis, B. L., Sundby, B., Lefrançois, L., Silverberg, N., and Nuzzio, D. B. (1998) Simultaneous measurement of O2, Mn, Fe, I-, and S(-II) in marine pore waters with a solid-state voltammetric microelectrode. Limnology and Oceanography, **43**(2), 325–333.

Mohanakrishnan, J., Gutierrez, O., Sharma, K. R., Guisasola, A., Werner, U., Meyer, R. L., Keller, J., and Yuan, Z. (2009) Impact of nitrate addition on biofilm properties and activities in rising main sewers. Water Research, **43**(17), 4225–4237.

Nakamura, Y., Satoh, H., Okabe, S., and Watanabe, Y. (2004) Photosynthesis in sediments determined at high spatial resolution by the use of microelectrodes. Water Research,

38(9), 2439–2447.
Okabe, S., Itoh, T., Satoh, H., and Watanabe, Y. (1999) Analyses of spatial distributions of sulfate-reducing bacteria and their activity in aerobic wastewater biofilms. Applied and Environmental Microbiology, **65**(11), 5107–5116.
Pages, A., Welsh, D. T., Teasdale, P. R., Grice, K., Vacher, M., Bennett, W. W., and Visscher, P. T. (2014) Diel fluctuations in solute distributions and biogeochemical cycling in a hypersaline microbial mat from Shark Bay, WA. Marine Chemistry, **167**, 102–112.
Pfeffer, C., Larsen, S., Song, J., Dong, M., Besenbacher, F., Meyer, R. L., Kjeldsen, K. U., Schreiber, L., Gorby, Y. a., El-Naggar, M. Y., Leung, K. M., Schramm, A., Risgaard-Petersen, N., and Nielsen, L. P. (2012) Filamentous bacteria transport electrons over centimetre distances. Nature, **491**(7423), 218–221.
Rabouille, C., Caprais, J. C., Lansard, B., Crassous, P., Dedieu, K., Reyss, J. L., and Khripounoff, A. (2009) Organic matter budget in the Southeast Atlantic continental margin close to the Congo Canyon: In situ measurements of sediment oxygen consumption. Deep-Sea Research Part II: Topical Studies in Oceanography, **56**(23), 2223–2238.
Revsbech, N. P., Jørgensen, B. B., and Blackburn, T. H. (1980) Oxygen in the sea bottom measured with a microelectrode. Science, **207**(4437), 1355–1356.
Sato, C., Nakayama, K., and Furukawa, K. (2012) Contributions of wind and river effects on DO concentration in Tokyo Bay. Estuarine, Coastal and Shelf Science, **109**, 91–97.
Schwermer, C. U., Ferdelman, T. G., Stief, P., Gieseke, A., Rezakhani, N., Van Rijn, J., De Beer, D., and Schramm, A. (2010) Effect of nitrate on sulfur transformations in sulfidogenic sludge of a marine aquaculture biofilter. FEMS Microbiology Ecology, **72**(3), 476–484.
Sugahara, S., Yurimoto, T., Ayukawa, K., Kimoto, K., Senga, Y., Okumura, M., and Seike, Y. (2010) A Simple in situ Extraction Method for Dissolved Sulfide in Sandy Mud Sediments Followed by Spectrophotometric Determination and Its Application to the Bottom Sediment at the Northeast of Ariake Bay. BUNSEKI KAGAKU, **59**(12), 1155–1161.
Valdemarsen, T., Kristensen, E., and Holmer, M. (2009) Metabolic threshold and sulfide-buffering in diffusion controlled marine sediments impacted by continuous organic enrichment. Biogeochemistry, **95**(2), 335–353.
Zhu, Q. and Aller, R. C. (2010) A rapid response, planar fluorosensor for measuring two-dimensional pCO2 distributions and dynamics in marine sediments. Limnology and Oceanography: Methods, **8**, 326–336.

TABLE 1. Average (maximum–minimum) percentage of sand, silt and clay by dry weight in sediment samples taken from three sites in Tokyo Bay between May 2010 and August 2011 (n = 9).

	Site 1	Site 2	Site 3
Sediment (particle size)			
Midium sand (0.425-0.850 mm)	3 (13 – 0)	6 (16 – 1)	0 (0 – 0)
Fine sand (0.106-0.425 mm)	5 (17 – 2)	46 (74 – 10)	1 (2 – 0)
Silt	71 (88 – 46)	32 (63 – 4)	82 (90 – 72)
Clay	20 (28 – 10)	15 (28 – 6)	17 (27 – 9)

TABLE 2. Physical and chemical properties of the surface sediment and bottom water at three sites in Tokyo Bay.

	Site 1			Site 2			Site 3		
	2010 July	2010 August	2011 August	2010 July	2010 August	2011 August	2010 July	2010 August	2011 August
Sediment (0-3 cm)									
AVS (mg g-dry^{-1})	0.8	1.0	1.3	1.8	1.2	1.1	3.3	2.3	2.6
LOI (%)	12	12	13	8	10	7	15	15	16
ORP (mV)	–329	–399	–387	–311	–299	–309	–411	–410	–388
Water content (%)	80	79	82	62	70	59	90	90	90
Tempetature (°C)	26	24	24	26	28	25	22	19	23
Bottom water									
DO (μM)	2	3	9	37	9	6	14	7	7
ORP (mV)	–124	–92	N.M.	+165	–18	N.M.	–125	–38	N.M.
Temperature (°C)	24	23	23	25	28	24	22	21	21
Salinity	27	32	34	26	27	33	29	33	35

N.M.: Not measured

AVS: Acid volatile sulfide

LOI: Loss of ignition

ORP: Oxidation-reduction potential

DO: Dissolved oxygen

TABLE 3. Local diffusive fluxes of T-H_2S (J(T-H_2S)), zone in which J(T-H_2S) was calculated, T-H_2S concentration at the sediment surface (Conc.) and ratio of the quantities of T-H_2S and $\Sigma(H_2S)$.

	Site 1				Site 2				Site 3			
	J(T-H_2S) (μmol cm^{-2} h^{-1})	Zone (mm)	Conc. (μM)	Ratio	J(T-H_2S) (μmol cm^{-2} h^{-1})	Zone (mm)	Conc. (μM)	Ratio	J(T-H_2S) (μmol cm^{-2} h^{-1})	Zone (mm)	Conc. (μM)	Ratio
July 2010	0.011	0 − 9.8	0	0.50	0		0	0	0.246	9.4 − 10.4	0	0.01
August 2010	0.121	0 − 2.0	201	0.50	0.011	3.0 – 30	0	1.21	0.146	0 − 2.0	109	0.26
August 2011	0.018	0 − 3.9	142	0.29	0.021	0 − 1.5	69	0.42	0.041	0 − 5.1	170	9.70

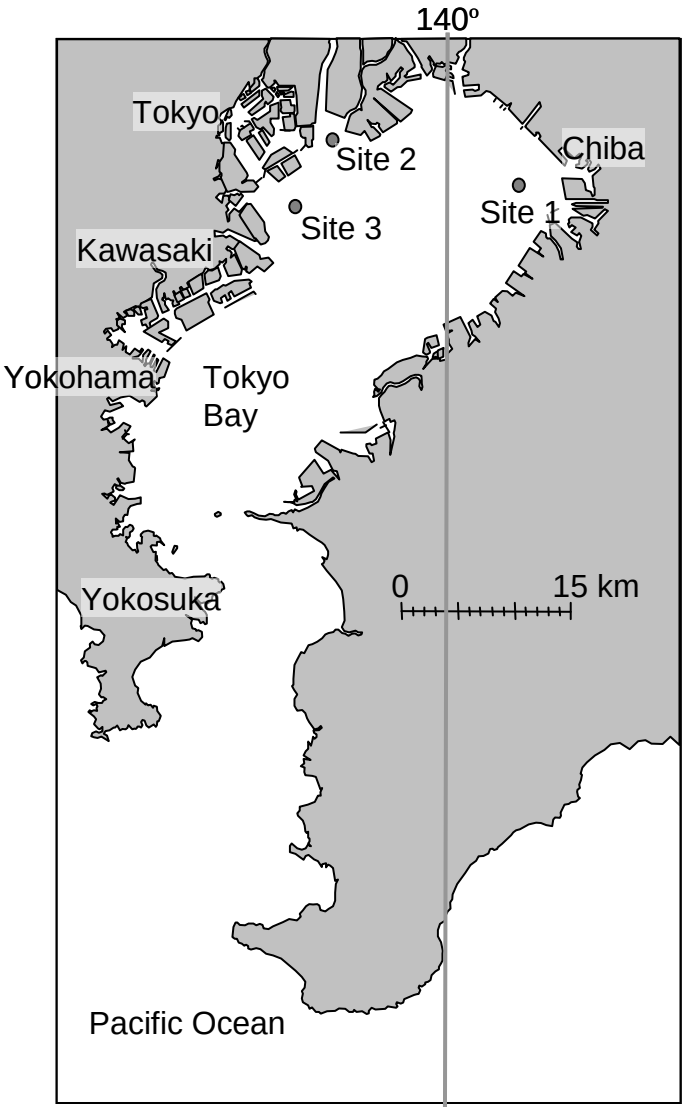

Rathnayake et al.

Figure 1. Map of Tokyo Bay and the location of the study sites.

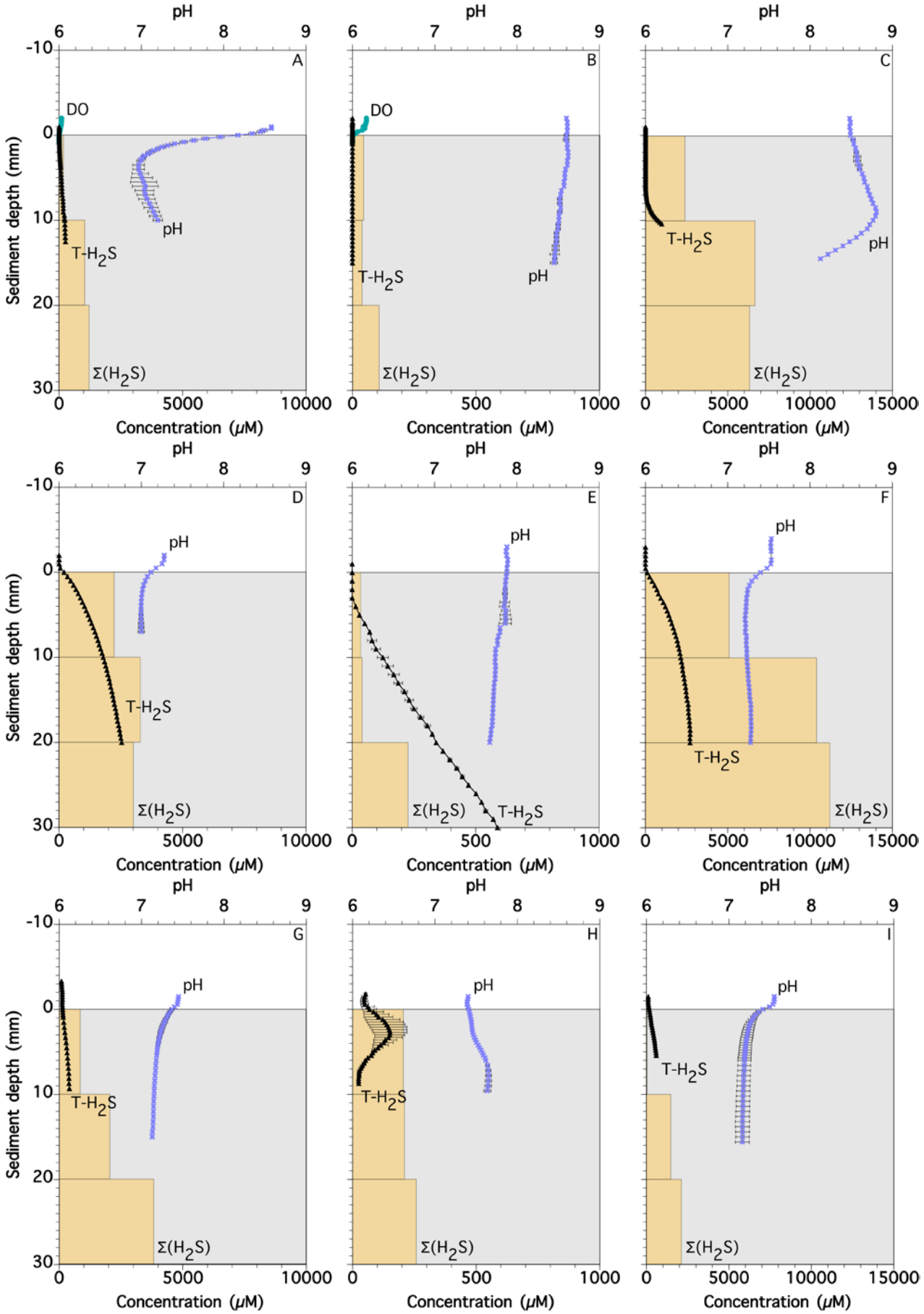

Rathnayake et al.

Figure 2. Vertical distribution of bulk $\Sigma(H_2S)$ (boxes) and concentration profiles of DO (filled circle), T-H_2S (filled triangle) and pH (cross) in the surface sediment of three study sites: Site 1 (A), Site 2 (B) and Site 3 (C) on July 2010; Site 1 (D), Site 2 (E) and Site 3 (F) on August 2010; and Site 1 (G), Site 2 (H) and Site 3 (I) on August 2011. Note that the maximal value of the horizontal axis is different among the study sites. The concentration profiles of DO, T-H_2S and pH are average values (n = 3) and error bars represent the standard deviations of triplicate measurements. Zero on the vertical axis corresponds to the surface of the sediment.

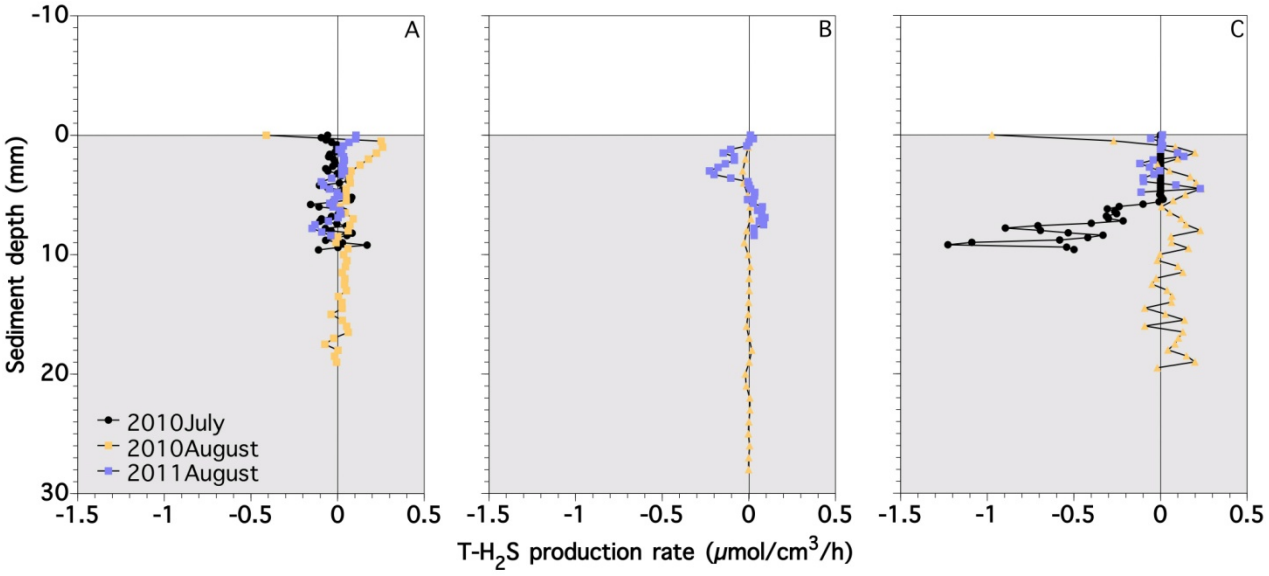

Rathnayake et al.

Figure 3. Vertical distribution and magnitude of the net volumetric T-H_2S production rates (*R*(T-H_2S)) in the sediment samples at Site 1 (A), Site 2 (B) and Site 3 (C). The rates were calculated based on the corresponding concentration profiles shown in Figure 2. Negative values indicate consumption. Zero on the vertical axis corresponds to the surface of the sediment.

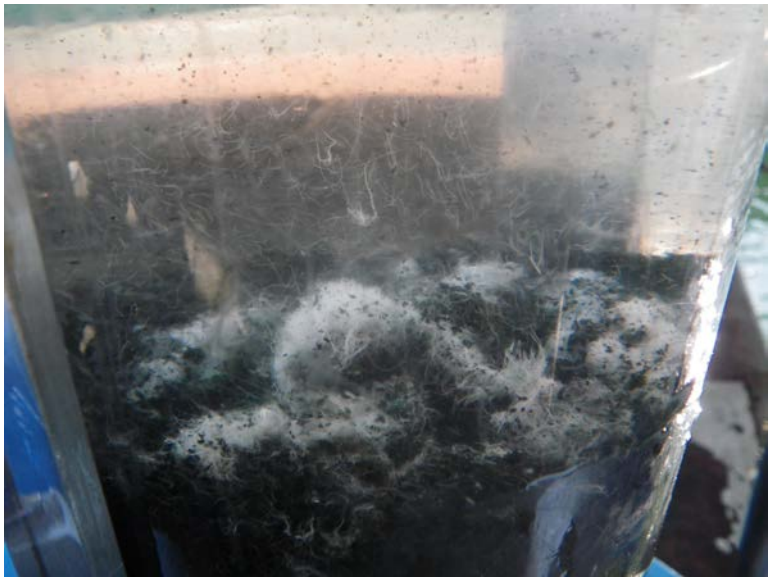

Figure 4. Photograph of the surface sediment sampled in Site 3 on July 2010. Inner diameter of the acrylic tube is 4 cm.